Modelling the Effect of Electrode Displacement on Transcranial Direct Current Stimulation (tDCS)

Sriharsha Ramaraju[1*], Mohammed A. Roula[1], Peter W. McCarthy[2]

[1] *Medical Electronics and Signal Processing Research Unit, University of South Wales, Treforest, CF37 1DL, United Kingdom*

[2] *Clinical Technology and Diagnostics Research Unit, University of South Wales, Trefforest, CF371DL, United Kingdom*

[*] *Corresponding Author: sriharsha.ramaraju@southwales.ac.uk*

Abstract

Objective: Transcranial Direct Current Stimulation (tDCS) is a neuromodulatory technique that delivers a low-intensity, direct current to cortical areas with the purpose of modulating underlying brain activity. Recent studies have reported inconsistencies in tDCS outcomes. The underlying assumption of many tDCS studies has been that replication of electrode montage equates to replicating stimulation conditions. It is possible however that anatomical difference between subjects, as well as inherent inaccuracies in montage placement, could affect current flow to targeted areas. The hypothesis that stimulation of a defined brain region will be stable under small displacements was tested.

Approach: Initially, we compared the total simulated current flowing through ten specific brain areas for four commonly used tDCS montages: F3-Fp2, C3-Fp2, Fp1-F4, and P3-P4 using the software tool COMETS. The effect of a slight (~1cm in each of four directions) anode displacement on the simulated regional current density for each of the four tDCS montages was then determined. Current flow was calculated and compared through 10 segmented brain areas to determine the effect of montage type and displacement. The regional currents, as well as the localised current densities, were compared with the original electrode location, for each of these new positions.

Results: Recommendations for montages that maximise stimulation current for the ten brain regions are considered. We noted that the extent to which stimulation is affected by electrode displacement varies depending on both area and montage type. The F3-Fp2 montage was found to be the least stable with up to 38% change in average current density in the left frontal lobe while the Fp1-F4 montage was found to the most stable exhibiting only 1% change when electrodes were displaced.

Significance: These results indicate that even relatively small changes in stimulation electrode placement appear to result in surprisingly large changes in current densities and distribution.

Keywords

Transcranial direct current stimulation (tDCS), current density, electrode displacement, computer simulation

1. Introduction

Transcranial Direct Current Stimulation (tDCS) is a neuromodulatory technique that delivers a low-intensity, direct current to cortical areas with the purpose of modulating the underlying brain activity [1-4]. The current is usually introduced into the cortex via a pair of sponge electrodes connected to a DC stimulator [5]. The use of direct current for stimulation began as early as the 18th century[6]. It saw little upsurge during 1960's but showed mostly inconsistent results [7-9]. Over the last decade, tDCS has grown as a popular research tool where it has been studied for effects on motor activities, depressive disorders, working memory, mathematical ability and risk-taking behaviour [10-14]. tDCS is thought to either enhance or inhibit the cortical excitability, an effect which apparently depends on the direction of current flowing through the cortical area. The direction of current itself depends on electrode position in relation to the targetted region of the cerebral cortex, as well as the surrounding morphology. It has been suggested that inhibitory effects occur when the cathode is directly above the targeted areas whereas excitatory effects occur when the targeted region is under the anode. However, the findings to date are less than convincing [1].

Behavioural effects of tDCS can be studied without a deep acquaintance with the underlying neurophysiology; however, it is still important to understand where the externally applied current is flowing exactly, the density of current injected by tDCS and whether there is sufficient current to influence the neural activity in the targeted region [2, 5]. It is currently impractical to non-invasively measure the total current flowing through a particular area of the brain. For that reason, well-constructed computer models can be a useful tool for simulating and, through this, understanding the pattern of current flow and relative current density induced by tDCS [15, 16]. Computational models could also play a major role in montage design, which has tended to be based more on either a general rule of thumb and experience or historical arrangements, rather than concrete evidence–based science. Computational models, if sufficiently detailed, can provide a more accurate insight into detailed current flow patterns and, in some cases, help by challenging the basic assumptions underpinning electrode placement [17]. One of the applications of computational models has been to test the effectiveness of montages [11, 17].

Based on previous work in this area [11, 12] and associated general assumptions [11, 12, 15], we hypothesised that displacement of target electrode from the stimulation point by 1cm in four directions (Table 1) should make a very minimal change. Although other studies [11, 15, 18] have looked at sensitivity analysis of electrode displacement, to our knowledge this is the first study to systematically explore the effect of anodal displacement on a range of commonly used tDCS montages. Our work has not only considered the change in current density values across the main simulated brain regions but also across voxels, in order to highlight localised stimulation patterns.

In order to study these displacement effects, COMETS, a MATLAB based toolbox [19], was used. COMETS has been previously used to investigate inconsistent outcomes of tDCS that may depend on anatomical differences [20] and optimal electrode positioning for inducing motor excitability changes in tDCS stimulation [21].

Table 1. Directional notations.

Displacement	**Direction of new position (looking perpendicularly above the original electrode position)**
Up	Electrode displaced upwards by 1cm in the same coronal plane as original position.
Down	Electrode displaced downwards by 1cm in the same coronal plane as original position.
Right	Electrode displaced right by 1cm in the same axial plane as original position.
Left	Electrode displaced left by 1cm in the same axial plane as original position.

2. Methods

The head model used in this simulation was extracted from standard Montreal Neurological Institute (MNI) brain atlas [22]. It uses a three-layer boundary element method (BEM) consisting of the scalp, skull boundaries and CSF (Cerebrospinal Fluid), as well as cortical surface model extracted from MRI T1 images of standard brain atlas using CURRY6 for Windows [19]. The model was tessellated with volumetric tetrahedral elements using the open-source mesh generation package TetGen (http://tetgen.belios.de) which is based on a constrained

Delaunay tetrahedralization (CDT) approach [23]. Well-known conductivity values for the scalp, skull and cerebral spinal fluid (CSF) were set as 0.22, 0.014 and 1.79 (S/m) respectively [24]. COMETS is based on Finite Element Modeling (FEM) in FORTRAN 90.

The cerebral cortex model consists of 26,012 voxels (vertices), each of which is associated with 3D coordinates. In this study, we segmented ten cortical regions of the brain by drawing boundaries around regions based on known anatomical maps. The segmented regions are left/right frontal (LF, RF), left/right motor (LM, RM), left/right parietal (LP, RP), left/right temporal (LT, RT), and left/right occipital (LO, RO). Fig 1 illustrates the 5 regions of left-cortex. The same regions can be assumed for the right cortex as well.

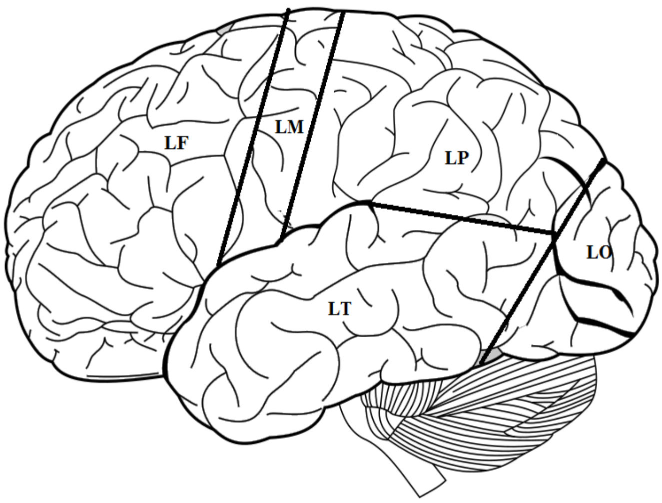

Fig 1. Five segmented regions of left cortex

Four commonly used tDCS montages (F3-Fp2 [12], C3-Fp2 [10], Fp1-F4 [25] and P3-P4 [13]) were considered for this study. The anode placement is placed on different regions of the cortex (Frontal lobe in F3-Fp2, motor cortex in C3-Fp2, prefrontal cortex in Fp1-F4 and parietal lobe in P3-P4 montage) in each of four montages. This not only introduces high variability of current induced across different regions of the brain but also elaborates the understanding of the current flow in those regions. The electrodes were placed as per 10-20 electrode system with a customised MATLAB script. In each electrode montage simulation, a direct current of 1.5mA was injected into the cortical surface using 5 x 7 cm electrode pads. For each montage used, the cortical surface was simulated five times with the cathode remaining in the same position whereas the anode was first kept at the original montage position, then displaced by 1 cm in one of the four directions; up, down, left or right when looking perpendicularly at the anode as illustrated in Table 1. Fig 2 explains the displacement using the F3-Fp2 montage as an example. The initial simulation for each montage was based on the anode being placed on the left dorsolateral prefrontal cortex (F3) whereas the cathode was located over the right supraorbital area (Fp2). In the next simulation, the cathode was at the same place (Fp2) whereas the anode was displaced to its left by 1 cm. This was followed by a further three simulations with the cathode position unchanged (Fp2) and the anode displaced from the original position [up, down and right in relation to its original position].

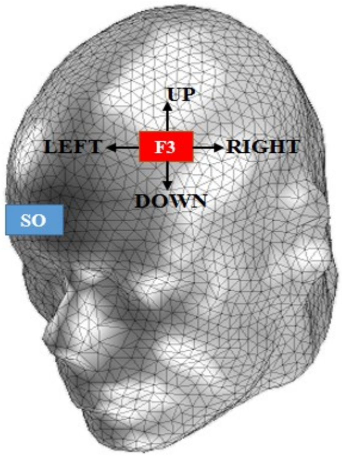

Fig 2. Model of the "head" indicating position of the anode electrode (at F3) and process of displacement by 1cm in either of the four directions (down, up, left and right) relative to its original "exact" location.

ASCII files generated at the end of every simulation contained current density values for each of the 26,012 voxels. These current density values were imported into MATLAB and mapped onto segmented cortical regions to determine the average current density per voxel across the regions of interest.

The magnitude of current density $|J_i|$ for voxel *i,* was calculated using the following formula.

$$|J_i| = \sqrt{(J_{i_x}^2 + J_{i_y}^2 + J_{i_z}^2)}$$

The average current density magnitude is defined as:

$$\overline{|J|} = \frac{\sum_{i=1}^{n} |J_i|}{n}$$

where *n* is the number of voxels in the considered region. Average current density $\overline{|J|}$ was calculated on each of the ten cortical areas considered. The results were divided into two sections: the effect of montage type and the effect of anodal displacement.

3. Results

3.1 Effect of montage type

Average regional current densities for each montage are summarised in Table 2. The largest values are highlighted in bold. The last column contains the montage that exhibits the highest average current density for the cortical region considered.

Table 2. The average current density values derived from the simulations across ten regions of the brain. The last column in the table indicates the montage found to have the largest current density.

	Average Current Density $\lvert \bar{J} \rvert$ (Am^{-2})				
Brain Region	**A:F3 C:Fp2**	**A:C3 C:Fp2**	**A:Fp1 C:F4**	**A:P4 C:P3**	**Montage with highest $\lvert \bar{J} \rvert$**
LF	0.22	**0.28**	0.14	0.07	A:F3 C:Fp2
RF	0.14	0.18	**0.22**	0.08	A:Fp1 C:F4
LT	0.05	**0.11**	0.05	0.09	A:C3 C:Fp2
RT	0.05	**0.08**	0.05	0.08	A:C3 C:Fp2
LP	0.07	0.21	0.04	**0.20**	A:C3 C:Fp2
RP	0.04	0.07	0.07	**0.19**	A:P4 C:P3
LO	0.03	0.06	0.03	**0.13**	A:P4 C:P3
RO	0.02	0.04	0.03	**0.12**	A:P4 C:P3
LM	0.15	**0.26**	0.09	0.12	A:C3 C:Fp2
RM	0.09	0.14	**0.16**	0.13	A:Fp1 C:F4

3.2 Effect of small anodal displacement

For the montage (F3-Fp2) in Fig.3 (a), the largest change in $\overline{|J|}$ of 38% and 34% was observed across areas LF and RF when the anode electrode was displaced downward by 1cm. $\overline{|J|}$ changed by 24% and 21% when the anode was displaced right by 1cm. A smaller change of 2% and 4% in $\overline{|J|}$ was observed in LF and RF respectively, when the anode was displaced upwards from the "exact" location.

For the montage (C3-Fp2) in Fig.3 (b), the largest change in $\overline{|J|}$ of 12% and 10% was observed across LM and RF respectively when the anode was displaced 1cm right of its location. Smallest changes of 4% and 8% in $\overline{|J|}$ were seen in LM and RF when anode was displaced to the left by 1cm.

For the montage (Fp1-F4) in Fig.3 (c), the largest change of 10% and 6% was observed in $\overline{|J|}$ across LF and RF when anode electrode was displaced towards down by 1cm. Smallest change of 4% and 1% was noticed in $\overline{|J|}$ across simulating areas when anode is displaced towards up.

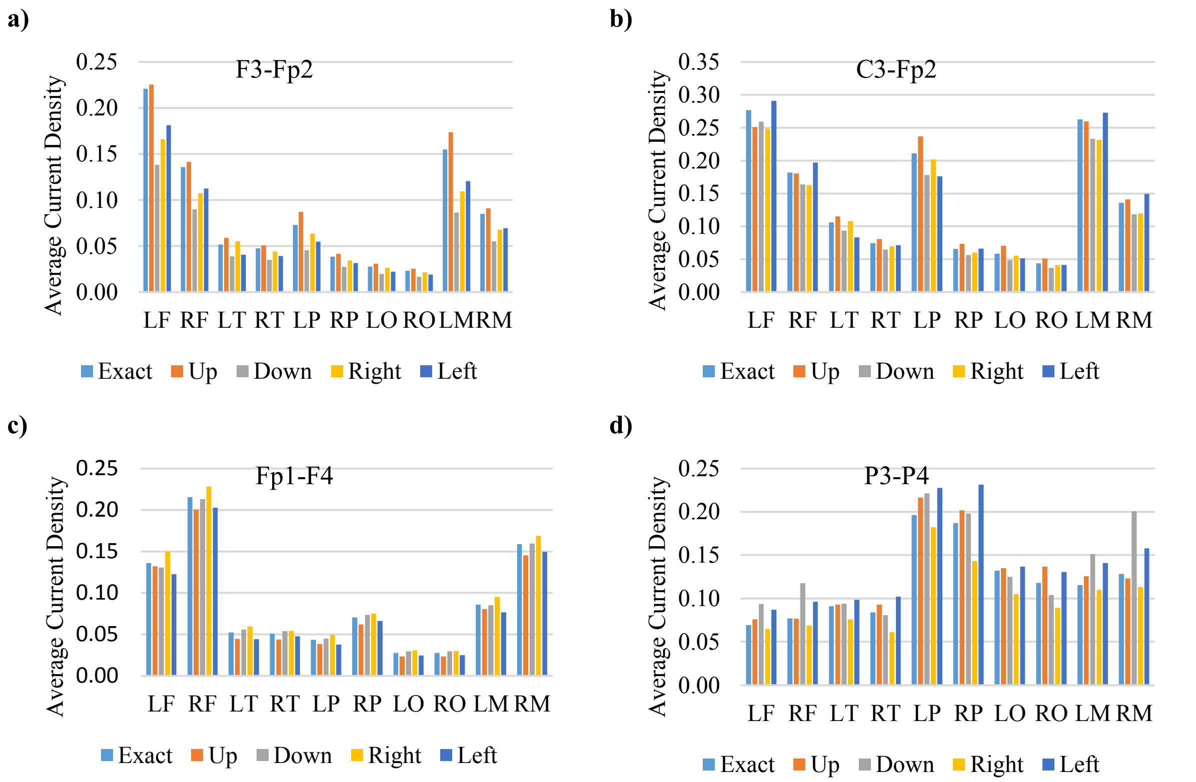

Fig 3. Demonstration of the effect of small changes in anodal placement on average current density over the 10 brain regions (LF,RF,LT,RT,LP,RP,LO,RO,LM,RM). This figure presents bar plots for: (a) F3-Fp2 montage with anode at F3; (b) C3-Fp2 montage with anode at C3; (c) Fp1-F4 montage with anode at Fp1 and (d) P3-P4 montage with anode at P3. Each bar plot illustrates the change in $\overline{|J|}$ values when the anode was displaced up, down, right and left respectively from the "exact" location, for each of the 4 conditions.

For montage (P3-P4) in Fig.3 (d), the largest change in $\overline{|J|}$ of 16% and 24% across simulated areas (LP-RP) was noticed when montage was displaced 1cm to the left of exact location. A smaller change of 10% and 8% was observed across simulating sites (LP-RP) when anode is displaced towards up.

Table 3. The minimum, average and maximum percentage change in $|J|$ across cortical voxels for each of the four montages.

Montage		Percentage change following displacement of anode in each of the four directions			
		Up	**Down**	**Right**	**Left**
F3-Fp2	Minimum	0	0	0	1
	Average	8	27	10	18
	Maximum	36	55	55	31
C3-Fp2	Minimum	0	0	0	0
	Average	10	12	6	8
	Maximum	55	29	24	45
Fp1-F4	Minimum	0	0	0	0
	Average	11	4	9	9
	Maximum	25	20	32	26
P3-P4	Minimum	0	0	0	0
	Average	9	18	15	21
	Maximum	50	100	39	68

3.3 Voxel-Level Effects

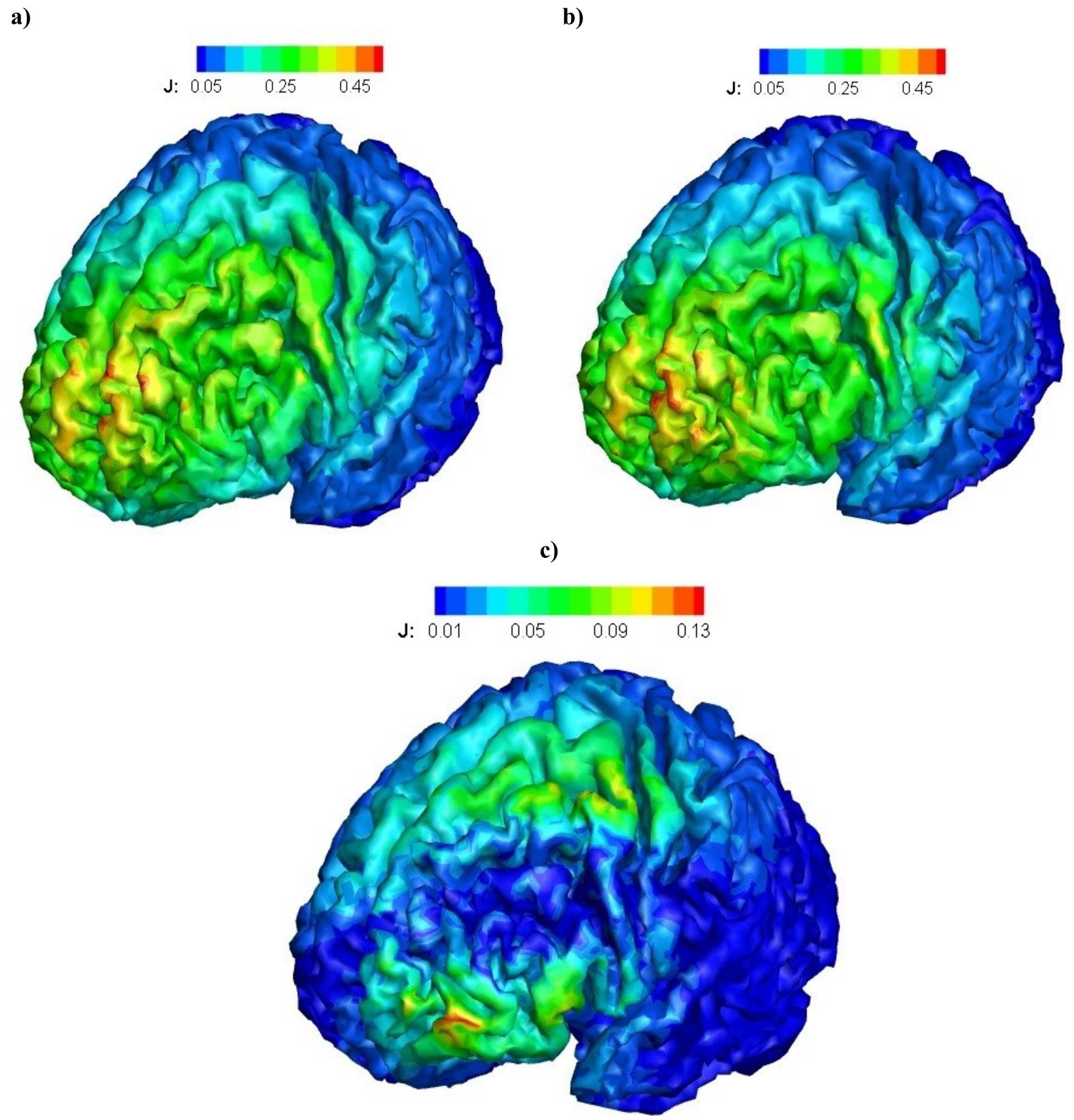

Fig 4. Current density distribution for (a) original F3-Fp2 montage (b) displaced F3-Fp2 montage, when the anode was displaced 1cm in the downward direction and (c) difference between the original and displaced montage current densities.

The effect of displacement was also calculated at the level of the individual voxel, from the 26012 voxels used, to identify the range (minimum, maximum) and average change seen. The results are summarised in Table 3. An example of colour coded voxel current densities is shown in Fig 4 corresponding to (a) the original F3-Fp2 montage, (b)1 cm anodal displacement downwards and (c) the voxel-wise difference between (a) and (b).

The overall displacement effect for each voxel in each of the four montages was calculated using Jaccard Index [26] and is summarised in Table 4. It calculates the relative overlap between segmented stimulated areas before and after displacement. Segmented areas are defined where current density > -3dB from peak current density value.

In the F3-Fp2 montage as an example, the Jaccard index is 22%, 35%, 31% and 40% (in the four displacement directions respectively). None of the other montages exhibited a higher than 50% index when displacement is applied. If the effect of displacement was minor, one would expect Jaccard Index values closer to 100%. This quantitative measure validate results shown above (Fig 4), namely that small displacements have a significant effect in stimulation spatial patterns within the cortex areas.

Table 4. Jaccard Index values for changes in simulated areas after displacement.

Montage	Up	Down	Right	Left
A:F3 C:Fp2	0.22	0.35	0.31	0.40
A:C3 C:Fp2	0.23	0.44	0.37	0.20
A:Fp1 C:F4	0.33	0.28	0.40	0.30
A:P3 C:P4	0.10	0.34	0.15	0.36

Furthermore, the current density was analysed based on its perpendicular and parallel components in relation to the cortical surface, in order to gauge if electrode displacement had any component specific effect. The normal current density of each displacement was found to be similar to the parallel current density of each displacement (Table 5). We note, however that in P4-P3 montage the percentage change of normal current density was more when compared to change in parallel current density across RP region and the percentage change in normal current density is less when compared to parallel current density across LP region when the electrode was displaced to the left.

Table 5. Percentage change in perpendicular (normal) and parallel currents across simulated regions when anode is displaced in four directions.

Montage	Simulated Region	Up		Down		Right		Left	
		Normal	Parallel	Normal	Parallel	Normal	Parallel	Normal	Parallel
F3-Fp2	LF	2.5%	2.2%	43.7%	37.4%	29.8%	24.8%	21.9%	17.8%
	RF	4.6%	4.0%	37.1%	33.8%	23.2%	20.9%	19.2%	17.2%
C3-Fp2	LM	2.0%	1.2%	16.7%	11.4%	17.6%	12.0%	6.4%	3.8%
	RM	4.9%	4.1%	15.1%	12.9%	13.7%	11.8%	12.1%	10.1%
Fp1-F4	LF	3.7%	3.1%	4.8%	4.0%	11.6%	9.9%	11.3%	9.9%
	RF	8.4%	7.0%	1.2%	1.0%	7.2%	5.9%	7.0%	5.9%
P4-P3	LP	1.4%	10.3%	2.7%	12.9%	6.3%	7.1%	1.6%	16.1%
	RP	12.1%	7.9%	14.9%	6.0%	29.7%	23.4%	40.1%	23.7%

4. Discussion

Expectedly, the regions directly under the simulated areas were found to have the highest current density values when compared to other regions. However, this was not always consistent. For instance, in the C3-Fp2 montage, the stimulated region C3 (left motor cortex (LM) or M1) was found to have a lower current density than the left frontal lobe (0.26 A/m^2 vs. 0.28 A/m^2 respectively). In the F3-Fp2 montage, stimulating the left frontal lobe (F3) induced a 0.22 A/m^2 $\overline{|J|}$ in that region, which resulted in 0.15 A/m^2 across the left motor cortex itself. Similarly, in the (Fp1-F4) montage, stimulating the left frontal lobe (Fp1) did not lead to increment of $\overline{|J|}$ in right motor cortex, but possibly because of the proximity of the cathode at F4 to the right motor cortex, it was found to have a higher current density (0.16 A/m^2). It is worth noticing that in all the three aforementioned montages, stimulating frontal lobe produced an increase in current density values across the motor cortex. A possible explanation could be the proximity of the motor cortex and frontal lobe regions in terms of current flow. In montage Fp1-F4, the stimulation site Fp1 is more distant to C3 than F4 is to C4 (right motor cortex), for this reason, the $\overline{|J|}$ value across the left motor cortex was only 0.09 A/m^2. The same appears to hold true for the first montage. Stimulating the parietal lobe in the fourth montage (P3-P4) produced higher current density values across motor cortex (LM & RM) and occipital lobe (LO, RO). This could be explained by the fact that the parietal lobe is located between these two regions. The results described above suggest that tDCS not only produces direct effects but also has the potential to produce un-anticipated indirect effects. This appears to have been seen in connectivity–driven changes of remote cortical and subcortical areas [27, 28]. tDCS is considered to modulate not only single neuronal and evoked neuronal activity, but also spontaneous neuronal oscillations [1]. Both modelling and animal studies have shown that networks of tightly coupled neurons can be more responsive to applied weak direct currents than neurons in isolation [29-31].

We initially hypothesised a negligible change in $\overline{|J|}$ values when the anodal electrode undergoes a displacement of 1cm. However, minimal changes of 4% and 1% were observed for C3-Fp2 and Fp1-F4 montages, changes of 38% and 24% were seen in the F3-Fp2 and P3-P4 montages respectively. The average change in $|J_i|$ values across all 26012 voxels for each displaced montage displacement was also large (when compared to average change across 26,012 voxels on C3-Fp2, Fp1-F4 montages the average change of 27% and 18% was observed across F3-Fp2 and P3-P4 montages respectively) .

These results indicate that even relatively small changes in stimulation electrode placement, which could imaginably be the consequences of human error during the montage fitting procedure, appear to be able to result in surprisingly large changes in current density in both regional and localised levels. Furthermore, if this simulation model is accurate, such changes may neither be linear nor symmetrical. To some extent in retrospect, this result could be expected due to the complex and anisotropic nature of the intricate geometry of the human brain. It is expected that more accurate models would reinforce this conclusion due further complexity and anisotropy introduced by the smaller structures and blood vessels.

A further area of complexity resides in the natural variability in human head size and cranial thickness variation both between individuals and across genders, with the average head size of 55.2cm for females and 57cm for males [32]. Furthermore, a significant relationship between brain size and type of connectivity also appears to have a substantial impact on current density distributions [33]. For instance, in the white matter tracts, where conductivity is anisotropic, the current flow might line up closer to the principal fibre direction. Another reason might be the presence and size of the gyri and sulci geometry, as studies have shown that electric current can concentrate on the edge of Gyri [34] and effects might not be homogenous throughout the stimulated area.

These factors might all be playing a role in determining the current densities across the different regions of the cortex. Therefore, placing the electrode at the same exact location on an individual should be strongly encouraged as slight displacement might cause noticeable changes in current density values and as a consequence reproducibility of the similar changes will not be seen. Although there are likely to be differences between individuals in relation to current flow and as a result areas affected, precision in the location of the stimulating electrode might help reduce the variation between subjects. A further suggestion might be to vary the position of the electrode slightly when performing the experiment, or use an adapted design to take variation into account, in order to determine whether location affects the outcome.

5. Conclusion

These results may explain the variability in outcomes of electrical stimulation studies. Such studies often assume they have performed the same experiment as they have used similar montages. Our results show that this may not be a sound assumption as similar montages can lead to large, even significant differences in regional stimulation due to errors that are well within experimental and morphological variations. We recommend therefore that imaging derived electrode positioning is considered in controlled electrical stimulation studies and alternatively that the protocol recognises the potential effects of positional variations in stimulating electrode positions.

6. Acknowledgement

S. Ramaraju does not have any conflict of interest. M.A. Roula does not have any conflict of interest. P. McCarthy does not have any conflict of interest. We would like to thank the University of South Wales for the centenary Ph.D. scholarship

References

1. Brunoni AR, Nitsche MA, Bolognini N, Bikson M, Wagner T, Merabet L, et al. Clinical research with transcranial direct current stimulation (tDCS): challenges and future directions. Brain stimulation. 2012;5(3):175-95.

2. Sadleir RJ, Vannorsdall TD, Schretlen DJ, Gordon B. Transcranial direct current stimulation (tDCS) in a realistic head model. Neuroimage. 2010;51(4):1310-8.

3. Izzidien A, Ramaraju S, Roula M, Ogeh J, McCarthy P, editors. The effect of tDCS on ERD potentials: A randomized, double-blind placebo controlled study. IEEE SSCI -CCMB,; 2014, Dec; Florida,: IEEE.

4. Ramaraju S, Izzidien A, Roula M, McCarthy P, editors. Effect of tDCS application on P300 potentials: A randomized, double blind placebo controlled study. IEEE SSCI-CCMB; 2014, Dec; Florida: IEEE.

5. Wagner T, Fregni F, Fecteau S, Grodzinsky A, Zahn M, Pascual-Leone A. Transcranial direct current stimulation: A computer-based human model study. Neuroimage. 2007;35(3):1113-24.

6. Zago S, Ferrucci R, Fregni F, Priori A. Bartholow, Sciamanna, Alberti: pioneers in the electrical stimulation of the exposed human cerebral cortex. The Neuroscientist. 2008;14(5):521-8.

7. Sheffield L, Mowbray R. The effects of polarization on normal subjects. Br. J. Psychiatry. 1968.

8. Hall KM, Hicks RA, Hopkins HK. The effects of low level DC scalp positive and negative current on the performance of various tasks. Br. J. Psychiatry. 1970.

9. Lolas F. Brain polarization: behavioral and therapeutic effects. Biol. Psychiatry. 1977;12(1):37-47.

10. Gandiga PC, Hummel FC, Cohen LG. Transcranial DC stimulation (tDCS): A tool for double-blind sham-controlled clinical studies in brain stimulation. Clin. Neurophysiol. 2006;117(4):845-50.

11. Bai S, Dokos S, Ho K-A, Loo C. A computational modelling study of transcranial direct current stimulation montages used in depression. Neuroimage. 2014;87:332-44.

12. Fregni F, Boggio PS, Nitsche M, Bermpohl F, Antal A, Feredoes E, et al. Anodal transcranial direct current stimulation of prefrontal cortex enhances working memory. Exp. Brain Res. 2005;166(1):23-30.

13. Kadosh RC, Soskic S, Iuculano T, Kanai R, Walsh V. Modulating neuronal activity produces specific and long-lasting changes in numerical competence. Curr. Biol. 2010;20(22):2016-20.

14. Fecteau S, Knoch D, Fregni F, Sultani N, Boggio P, Pascual-Leone A. Diminishing risk-taking behavior by modulating activity in the prefrontal cortex: a direct current stimulation study. J. Neurosci. 2007;27(46):12500-5.

15. Datta A, Baker JM, Bikson M, Fridriksson J. Individualized model predicts brain current flow during transcranial direct-current stimulation treatment in responsive stroke patient. Brain stimulation. 2011;4(3):169-74.

16. Miranda PC, Lomarev M, Hallett M. Modeling the current distribution during transcranial direct current stimulation. Clin. Neurophysiol. 2006;117(7):1623-9.

17. Bikson M, Rahman A, Datta A. Computational models of transcranial direct current stimulation. Clin. EEG Neurosci. 2012;43(3):176-83.

18. Dmochowski JP, Datta A, Huang Y, Richardson JD, Bikson M, Fridriksson J, et al. Targeted transcranial direct current stimulation for rehabilitation after stroke. Neuroimage. 2013;75:12-9.

19. Jung Y-J, Kim J-H, Im C-H. COMETS: a MATLAB toolbox for simulating local electric fields generated by transcranial direct current stimulation (tDCS). Biomed. Eng. Lett. 2013;3(1):39-46.

20. Kim J-H, Kim D-W, Chang WH, Kim Y-H, Kim K, Im C-H. Inconsistent outcomes of transcranial direct current stimulation may originate from anatomical differences among individuals: Electric field simulation using individual MRI data. Neurosci. Lett. 2014;564:6-10.

21. Lee M, Kim Y-H, Im C-H, Kim J-H, Park C-h, Chang WH, et al. What is the optimal anodal electrode position for inducing corticomotor excitability changes in transcranial direct current stimulation? Neurosci. Lett. 2015;584:347-50.

22. Collins DL, Neelin P, Peters TM, Evans AC. Automatic 3D intersubject registration of MR volumetric data in standardized Talairach space. J. Comput. Assist. Tomogr. 1994;18(2):192-205.

23. Si H. Adaptive tetrahedral mesh generation by constrained Delaunay refinement. International Journal for Numerical Methods in Engineering. 2008;75(7):856-80.

24. Haueisen J, Ramon C, Eiselt M, Brauer H, Nowak H. Influence of tissue resistivities on neuromagnetic fields and electric potentials studied with a finite element model of the head. IEEE Trans. Biomed. Eng. 1997;44(8):727-35.

25. Knoch D, Nitsche MA, Fischbacher U, Eisenegger C, Pascual-Leone A, Fehr E. Studying the neurobiology of social interaction with transcranial direct current stimulation—the example of punishing unfairness. Cereb. Cortex. 2008;18(9):1987-90.

26. Huang Y, Dmochowski JP, Su Y, Datta A, Rorden C, Parra LC. Automated MRI Segmentation for Individualized Modeling of Current Flow in the Human Head. Journal of neural engineering. 2013;10(6):10.1088/741-2560/10/6/066004.

27. Boros K, Poreisz C, Münchau A, Paulus W, Nitsche MA. Premotor transcranial direct current stimulation (tDCS) affects primary motor excitability in humans. Eur. J. Neurosci. 2008;27(5):1292-300.

28. Lang N, Siebner HR, Ward NS, Lee L, Nitsche MA, Paulus W, et al. How does transcranial DC stimulation of the primary motor cortex alter regional neuronal activity in the human brain? Eur. J. Neurosci. 2005;22(2):495-504.

29. Parra LC, Bikson M, editors. Model of the effect of extracellular fields on spike time coherence. Engineering in Medicine and Biology Society, 2004. IEMBS'04. 26th Annual International Conference of the IEEE; 2004: IEEE.

30. Deans JK, Powell AD, Jefferys JG. Sensitivity of coherent oscillations in rat hippocampus to AC electric fields. J. Physiol. 2007;583(2):555-65.

31. Fröhlich F, McCormick DA. Endogenous electric fields may guide neocortical network activity. Neuron. 2010;67(1):129-43.

32. Bushby KM, Cole T, Matthews JN, Goodship JA. Centiles for adult head circumference. Arch. Dis. Child. 1992;67(10):1286-7.

33. Hänggi J, Fövenyi L, Liem F, Meyer M, Jäncke L. The hypothesis of neuronal interconnectivity as a function of brain size—a general organization principle of the human connectome. Front. Hum. Neurosci. 2014;8:915.

34. Datta A, Bansal V, Diaz J, Patel J, Reato D, Bikson M. Gyri –precise head model of transcranial DC stimulation: Improved spatial focality using a ring electrode versus conventional rectangular pad. Brain stimulation. 2009;2(4):201-7.